Experiments and Analysis for Fractional Order Modelling of an EEG Recording Process

Guillaume Becq, Alina Voda, Gildas Besançon, Pierre-Olivier Amblard and Olivier Michel
Univ. Grenoble Alpes, GIPSA-Lab, F-38000 Grenoble, France
CNRS, GIPSA-Lab, F-38000 Grenoble, France

Keywords: Constant Phase Element, CPE, EEG, Electroencephalogram, Fractional Order System, Frequency-based Identification, Head Phantom, Impedance Spectroscopy.

Abstract: In this study, an original experimental setup is proposed to analyze the transfer function of an electroencephalographic (EEG) measurement chain: this setup allows to control electrodes inserted into an electrolytic medium, and observe the electrical potentials at different points with electrodes connected to an electroencephalographic recording system. Experimental transfer functions are obtained that enable to characterize the influence of the electrolyte, the electrode-electrolyte interfaces, and the medium itself. A theoretical model containing so-called *constant phase elements* is then proposed and analysed to understand the behaviour of the transfer function in Bode or Nyquist representations. Experimental and theoretical systems are finally compared.

1 INTRODUCTION

Electroencephalographic recorders (EEG) are widely used in hospital or experimental protocols and their basic principles are described in several textbooks (Cooper et al., 1969), (Nunez and Srinivasan, 2006). They are nowadays simple to use and make possible the recordings of huge amounts of data necessary to observe neural activities, diagnose diseases or understand brain functions. They have a good temporal resolution and can be used to have a precise spatial location, as in intracranial stereotaxic recordings for example. However, depending on the electrodes used to measure neural activities, such as silver electrodes on the scalp, or platinum electrodes on the intracranial recordings for instance, the recorded signals are not the same in terms of amplitudes and dynamics.

Several studies have emphasized a modification of the amplitude according to laws varying with *non integer* powers of the frequency (Boonstra et al., 2009), (Miller et al., 2009), (Logothetis et al., 2007), (Bédard and Destexhe, 2009), (Dehghani et al., 2010), (Ragheb and Geddes, 1990), (Becq et al., 2008), (Magin et al., 2011) by incriminating different parts of the observed systems: some of them show that it is due to neuronal activities, other ones that this is due to the metallic electrodes, or finally that this can come from the propagation medium.

In order to understand the influence of each part of the system, experimental rigs can be tested. Among them, so-called *head phantoms* have been developed to mimic EEG measurements of brain signals inside a head. As presented in (Leahy et al., 1998), several systems such as cadaver heads, gelatin filled skulls, or other chemical materials have been used to reproduce the media of the head; dipoles are proposed to generate the signals mimicking the activity of a brain area and currents of $1\,s$, $10\,Hz$ sine waves are driven into the conductor to evaluate the recordings. In (Baillet et al., 2001), a similar setup is used with a $5\,Hz$ sinusoid. In (Collier et al., 2012), an even more realistic head phantom is used with a $10\,Hz$, $30\,s$, $6.2\,V$ peak-to-peak sine signal applied. In all these studies, the devices enable to study the performances of source localization algorithms. However, the dynamical properties of the different parts of the system are not taken into account, and since impedances of the biological tissues depend on frequencies, as described in (Schwan and Foster, 1980) for example, it is hard to evaluate the transfer function of the whole system. Besides, the impedances of the electrode-electrolyte interfaces, which are of high importance in electrophysiology (Geddes, 1997), is not taken into account. Modelisations of such systems with fractional order systems are proposed in (Magin and Ovadia, 2010) and (Magin et al., 2011). Finally, nothing is said about the effect of using elevated potentials on the electrodes, that leads to reduction-oxidation re-

Becq, G., Voda, A., Besançon, G., Amblard, P-O. and Michel, O.
Experiments and Analysis for Fractional Order Modelling of an EEG Recording Process.
DOI: 10.5220/0006417905590566
In *Proceedings of the 14th International Conference on Informatics in Control, Automation and Robotics (ICINCO 2017) - Volume 1*, pages 559-566
ISBN: 978-989-758-263-9

actions, sources of physical phenomenons which can transform electrodes and electrolytes.

In this article, an original experimental rig is proposed to characterize the transfer function of the medium and its coupling with the electrodes at different frequencies. To that end, electrical potentials are applied on electrodes inserted into a medium. Electrical potentials are chosen in a range that do not induce reduction-oxidation reactions at the electrode-electrolyte interfaces. Signals are collected on an EEG recorder, via other electrodes also inserted into the medium. In this article, the influence of two different media, an electrolyte or a sponge wet with an electrolyte, are compared. An electrical circuit including so-called *Constant Phase Elements* (CPE) (Diard et al., 2013), (Jorcin et al., 2006), (Zoltowski, 1998) in order to capture the non-integer order of the system is proposed and its theoretical transfer function and properties are calculated. This enables to fit the experimental data and identify the parameters of the theoretical proposed system, from the arc paths of the transfer functions observed in the Nyquist representations.

The article is constructed as follows: first the experimental setup and related empirical transfer function estimates are presented in section 2. Then, the theoretical transfer function based on a proposed electrical circuit is studied in section 3 and compared with the experimental recordings. Results are discussed in section 4 before concluding.

2 EXPERIMENTAL SETUP, MEASURES & ANALYSIS

2.1 Description of the Experimental Setup

The general setup proposed for testing the EEG recorder is described in Fig. 1: in short, signals are simulated on a computer (Simu) and sent to a digital-to-analog converter (DAC) as voltage inputs applied to electrodes. These inputs electrodes (Elec in) are inserted into a medium (Med). Output electrodes (Elec out) are also inserted into the medium to record some signals. Input and output values on the medium are recorded with an EEG recorder (EEG rec). According to linear system theory, the system is reduced to Fig. 1. e) with different transfer functions H_i from the simulation into an input electrode X_{in} to a recording electrode X_i.

The DAC is a National Instruments CRIO-9263, voltage analog output module with 4 outputs, 16 bits, 100 KS/s per channel, mounted on a cDAQ-9181 ethernet chassis. Signals are simulated in Python with Scipy modules (Jones et al., 2016). They are binded to an own-purpose library in C linked to the National Instruments library interfacing the DAC. Python and C codes are available in (Becq, 2016).

Home-made pure platinum electrodes are used in this study in order to avoid reduction–oxidation reactions at the contact of the electrodes with electrolytic solutions for potentials lower than $E^{\circ}_{Pt} = 1.2\,V$ at $25^{\circ}\,C$ (Didier, 1984). Each electrode consists of a thin cylinder of platinum with a diameter of $0.5\,mm$ and a length of $1\,cm$, soldered on a copper wire. The solder junction is covered by a thin layer of epoxy resin for insulation.

Two media are tested to compare their influences on the system: an electrolytic solution; a sponge fully wet with an electrolytic solution. The electrolyte solution is obtained from the dissolution of a tablet of phosphate buffered saline (PBS) into pure water. A synthetic tiler foam grout sponge, with dimensions 15.5 by 10.5 by 5.2 cm is used to test the influence of a propagation medium. The sponge is washed with pure water between experiments. The sponge, or the solution, is contained in a home-made basin made of polyethylene terephthlate glycol-modified (PETG) slices stuck together with a silicon glue, as seen in Fig. 1. This setup is simple, cheap and very convenient for working with liquids. PBS is a P4417 Sigma-Aldrich reference. The basic dissolution is one tablet in $200\,ml$ of pure water. The dissolution used in this study is $1/2$ tablet in $1\,l$ of pure water, so as to obtain a weakly conductive solution. The temperature of the room is checked with a thermometer and is about 24 to $25^{\circ}\,C$.

Electrodes are inserted into the sponge or liquid on a depth of approximatley $0.5\,cm$. Electrodes are linearly spaced on 6 locations with $d_{1,2} = 1\,cm$, $d_{1,3} = 3\,cm$, $d_{1,4} = 5\,cm$; $d_{1,Ref} = 6\,cm$; $d_{1,GND} = 8\,cm$ with the input electrode in 1; the output electrodes are in 2, 3 and 4; the ground electrode (GND) is common to the EEG recorder and the ADC; the reference electrode of the EEG recorder is set in Ref; electrode 1 is also connected to the EEG recorder.

The EEG recorder is a g.tec g.USBamp, with an input voltage range of $\pm 250\,mV$, no highpass filter, a lowpass at $6.6\,kHz$, an input impedance $> 10^{10}\,\Omega$, an analogic to digital conversion resolution of $24\,bits$ with a maximal sampling frequency of $38.4\,kHz$ per channel, and 16 channels. Signals are recorded at $4.8\,kHz$ in this study.

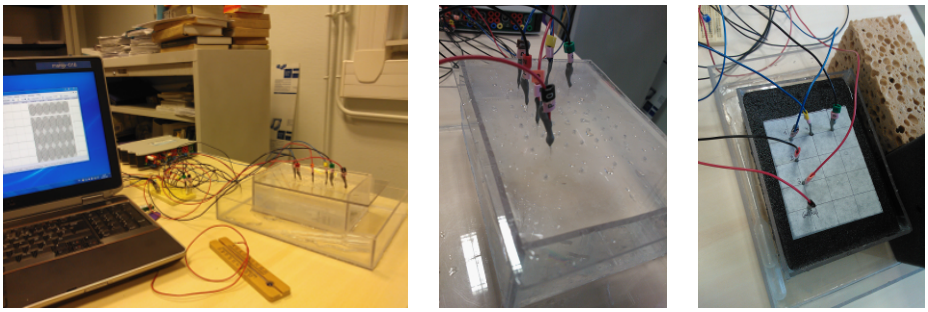

a) b) c)

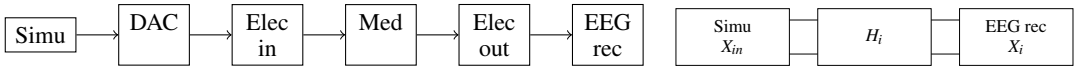

d) e)

Figure 1: Illustration of the proposed experimental setup for EEG recorder testing with different representations. a) Overall view of the setup; b) Electrolytic solution and electrode positioning; c) Sponge experiment and positioning; d) Scheme of the setup. e) Scheme of one equivalent system H_i for one input electrode X_{in} and one recording electrode X_i.

2.2 Experimental Transfer Functions Estimates and Analysis

Empirical transfer function estimates (ETFE) (Ljung, 1987) are obtained by impedance spectroscopy (Al-Nazer et al., 2013) either by generating with the computer a sequence of sine waves with amplitude varying from -0.1 to 0.1 V at different frequencies, [0.1, 0.125, 0.25, 0.5, 1, 2, 4, 8, 10, 16, 32, 64, 100, 128] Hz, or by using a reproducible sequence of white Gaussian noise with mean 0 V and standard deviation 0.1 V. For all methods the ETFE is the ratio between the output signal over the input signal at different frequencies. When working with pure frequencies, sequences of at least 10 periods are recorded and the evaluation is made after removing transients, generally the first cycle of the trial for low frequencies. The ETFE is obtained by dividing the Fourier coefficients of the signals at the different frequencies of interest:

$$\hat{H}_i(f) = \frac{\hat{X}_i(f)}{\hat{X}_{in}(f)}$$

When working with white noise, a sequence of 100 s is used. Half a second at the beginning and end of the sequence are removed for data processing. A method similar to Welch windowing (Welch, 1967) with non overlapping windows of 1 s, 4800 samples, is applied to estimate the Fourier coefficients $X_i(f)$ of each signal $x_i(t)$ for each frequency of interest. The ETFE $\hat{H}(f)$ is the mean of the ratio of these Fourier coefficients obtained on windows indexed by k:

$$\hat{H}_i(f) = \frac{1}{N}\sum_{k=1}^{N}\frac{\hat{X}_{i,k}(f)}{\hat{X}_{in,k}(f)}$$

The empirical transfer functions obtained with impedance spectroscopy on an electrolyte (e) or on the sponge wet with the electrolyte (s) are represented in the Bode and Nyquist representations of Fig. 2.

On all electrodes the transfer functions show behaviors of high pass filters. For the electrolyte alone (e, red color), differences are observed on the Bode amplitudes that decrease with distances from the electrodes to the input. There is no modification of the Bode phase with distances. Arcs are observed on the Nyquist representation with varying centers and radii. The same behaviors are observed with the sponge wet with an electrolyte (s, blue color). On the Bode representation, amplitudes are higher with s. The white noise estimates show less variance with s. On the Nyquist plot, dispersion of point clouds seems less important with s. On the Bode representation, there is a small shift in phase angle between the two media. In the Nyquist representation and especially in (d), there are slight differences in the tangents at the origin at low frequencies, and always differences in the real part at high frequencies.

These behaviors looks like transfer functions of a first order high pass filters but with several differences: slopes of the attenuations of the amplitude at low frequencies on the Bode representations are less than -20 dB / dec; the limits of the phases at low frequencies in the Bode representations tend to a value smaller than $\frac{\pi}{2}$; the path in the Nyquist representation is an arc but the center of this arc is not on the real axis; equivalently, the path at the origin is not tangent to the imaginary axis. In order to understand these behaviors, a theoretical model based on constant phase elements is proposed in the next section.

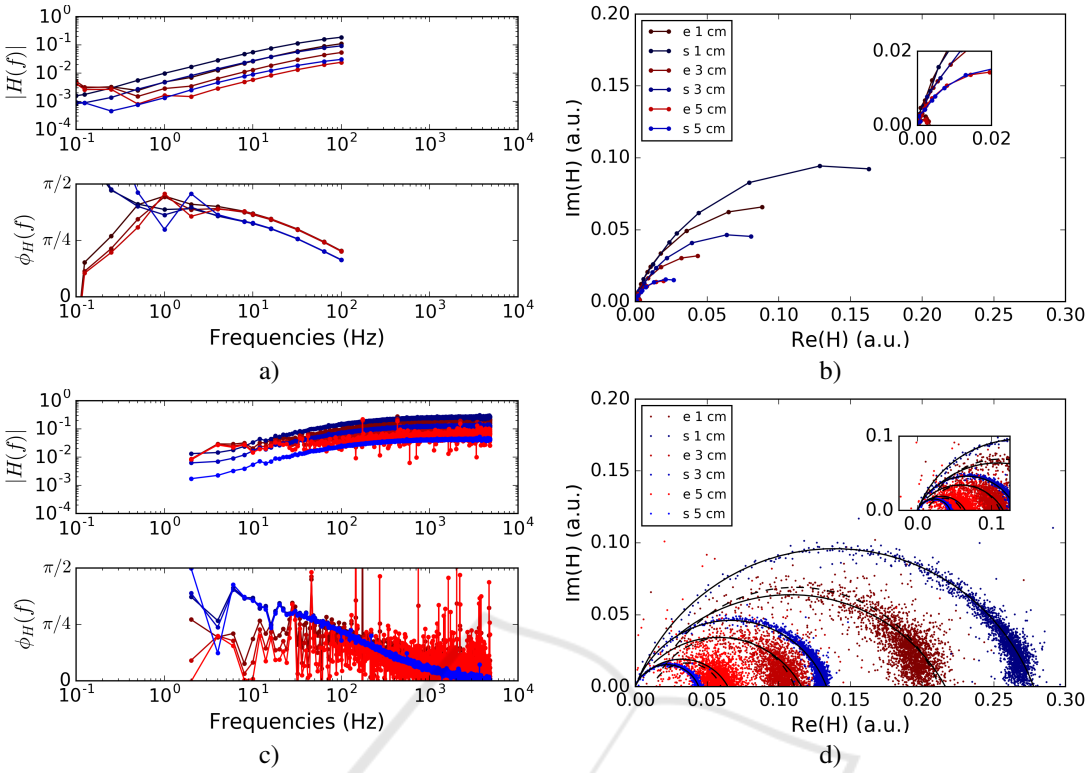

Figure 2: Empirical transfer functions estimated at different frequencies for the electrolyte alone (e) or the sponge wet with the electrolyte (s): a) b) with sinusoid; c) d) with white noise; a) c) Bode plot of the transfer function for the electrodes 2, 3 and 4 at distances 1, 3, and 5 cm from electrode 1. Magnitudes (up) and phases (bottom) of the transfer functions are given in function of the frequencies in Hz. b) d) Nyquist representation of the transfer function in arbitrary unit (a. u.). Fits, with theoretical paths presented in section 3, are represented with black curves on d). All systems show general behaviors of high pass filters.

3 THEORETICAL MODELLING WITH CONSTANT PHASE ELEMENTS

In the rest of the paper, $X(p)$ and $X(\omega)$ are used to represent the Laplace and Fourier transform of signal $x(t)$ with time t.

3.1 Constant Phase Elements and General Models

Let us start with the simple model of impedance $Z(\omega)$ of a constant phase element, as given in (Diard et al., 2013), (Jorcin et al., 2006), (Zoltowski, 1998):

$$Z(\omega) = \frac{1}{Q(j\omega)^{\alpha}} = \frac{1}{Q\omega^{\alpha}} \exp(-j\alpha\frac{\pi}{2}) = \frac{1}{Q\omega^{\alpha}}(c_{\alpha} - js_{\alpha})$$

with $c_{\alpha} = \cos\left(\alpha\frac{\pi}{2}\right)$ and $s_{\alpha} = \sin\left(\alpha\frac{\pi}{2}\right)$.

The phase of this component is $\phi_Z = -\alpha\frac{\pi}{2}$, is constant, and explains its name. We replace resistors with CPE components in voltage dividers generally used to obtain first order high pass filters. Other complex circuits with CPE can be found in (Diard et al., 2013).

The general electrical scheme for a potential or voltage divider is given in Fig. 3. a).

It is supposed that the input resistance when measuring X_2 is high as compared to Z_2. In this case, the impedance $Z(p)$ of the equivalent circuit from $X_1(p)$ and the transfer function $H(p) = \frac{X_2(p)}{X_1(p)}$ are related by:

$$H(p) = Z_2(p)Z^{-1}(p), \text{ or } Z(p) = Z_2(p)H^{-1}(p)$$

If $Z_2(p) = R$, the relation between Z or H, depending on the measurement made on the system is given by:

$$\begin{array}{ll} |Z(p)| = \frac{R}{|H(p)|} & \phi_{Z(p)} = \exp(-j\phi_H(p)) \\ |H(p)| = \frac{R}{|Z(p)|} & \phi_{H(p)} = \exp(-j\phi_Z(p)) \end{array} \quad (1)$$

For $Z_2(p) = R$ and $Z_1(p) = 1/(jC\omega)$, the system is a high pass filter of the first order.

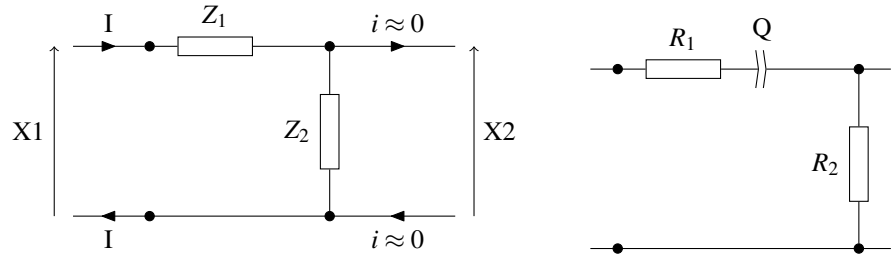

Figure 3: Examples of voltage divider: a) general model, b) resistive and high pass filter with CPE.

3.2 Introducing a Constant Phase Element in a High Pass Filter

The proposed circuit to obtain a high pass filter with a CPE is given in Fig. 3 b). This model is proposed to take into account a resistive component in the medium and a CPE that summarizes the electrode-electrolytic interfaces for the input electrode X_{in} and output electrode X_i. The development of the transfer function leads to:

$$H(\omega) = \frac{R_2}{R_1 + R_2 + \frac{1}{Q(j\omega)^\alpha}} = \frac{R_2 Q (j\omega)^\alpha}{(R_1+R_2) Q (j\omega)^\alpha + 1}$$

Let $A(\omega) = R_2 Q \omega^\alpha = A\omega^\alpha$ with $A = R_2 Q$ and $A_*(\omega) = (R_1+R_2) Q \omega^\alpha = A_* \omega^\alpha$.

$$H(\omega) = \frac{A(\omega)(c_\alpha + j s_\alpha)}{(A_*(\omega)(c_\alpha + j s_\alpha) + 1)}$$

$$H(\omega) = \frac{A(\omega)\,(A_*(\omega) + c_\alpha)}{B_*(\omega)} + j\frac{A(\omega) s_\alpha}{B_*(\omega)}$$

$$B_*(\omega) = 1 + 2A_*(\omega) c_\alpha + A_*^2(\omega)$$

$$H(\omega) = C(\omega)(A_*(\omega) + c_\alpha) + jC(\omega) s_\alpha \quad (2)$$

Where $C(\omega) = A(\omega)/B_*(\omega)$

Let f be the frequency such that $\omega = 2\pi f$. On one hand, if the real part of the transfer function is denoted by x and the imaginary part by y, which corresponds to the respective axes in the Nyquist representation, the path of the transfer function $H(f)$ can be given in its parametric form with:

$$\begin{cases} x(f) &= C(f)(A_*(f) + c_\alpha) \\ y(f) &= C(f) s_\alpha \end{cases} \quad (3)$$

On a second hand, the equation of a circle centered at C with coordinates (x_C, y_C) and radius r is given by:

$$x^2 - 2x_C x + x_C^2 + y^2 - 2y_C y + y_C^2 - r^2 = 0 \quad (4)$$

Let $a = R_2 Q (2\pi)^\alpha$, $a_* = (R_1+R_2) Q (2\pi)^\alpha$, and $u = f^\alpha$. Combinations of the terms of the parametrization (3) yields:

$$x^2 + y^2 = \frac{a^2 u^2}{1 + 2a_* u c_\alpha + a_*^2 u^2}$$

$$-2x_C x - 2y_C y = -2\frac{x_C a u (a_* u + c_\alpha) + y_C (a u s_\alpha)}{1 + 2a_* u c_\alpha + a_*^2 u^2}$$

Substituting these expressions in the circle equation (4) gives:

$$a^2 u^2 - 2x_C a u (a_* u + c_\alpha) - 2y_C (a u s_\alpha) + \\ + (x_C^2 + y_C^2 - r^2)(1 + 2a_* u c_\alpha + a_*^2 u^2) = 0$$

Developing and reordering the terms in function of the order of u yields:

$$\left(a^2 - 2aa_* x_C + a_*^2 (x_C^2 + y_C^2 - r^2)\right) u^2 + \cdots \\ \cdots + (-2ac_\alpha x_C - 2as_\alpha y_C + \cdots \\ \cdots + (x_C^2 + y_C^2 - r^2) 2a_* c_\alpha) u + \cdots \\ \cdots + (x_C^2 + y_C^2 - r^2) = 0$$

If parametrization (3) follows a circle, this must be satisfied for all u. This leads to the resolution of the system:

$$a^2 - 2aa_* x_C + a_*^2 (x_C^2 + y_C^2 - r^2) = 0 \quad (5)$$

$$-2ac_\alpha x_C - 2as_\alpha y_C + (x_C^2 + y_C^2 - r^2) 2a_* c_\alpha = 0 \quad (6)$$

$$(x_C^2 + y_C^2 - r^2) = 0 \quad (7)$$

Using Eq. (7) in Eq. (5) gives: $a^2 - 2aa_* x_C = 0$ which implies:

$$x_C = \frac{a}{2a_*} \quad (8)$$

Using Eq. (7) in Eq. (6) and Eq. (8) gives:

$$c_\alpha x_C + s_\alpha y_C = 0$$

$$y_C = -\frac{a}{2a_*}\frac{c_\alpha}{s_\alpha} = -\frac{x_C}{\tan(\alpha\frac{\pi}{2})} \quad (9)$$

Finally, Eq. (8) and (9) in Eq. (7) yield:

$$r = \frac{1}{2}\frac{a}{a_*}\frac{1}{s_\alpha} = \frac{x_C}{s_\alpha} \quad (10)$$

This proves that the parametrization (3) follows a circle. One can notice that the ratio $\rho = \frac{a}{a_*} = \frac{R_2}{R_1+R_2}$ does not depend on Q, and that the location of x_C depends only on this ratio. In addition, we also have the simple rules $x_C = s_\alpha r$ and $y_C = -c_\alpha r$. At low frequencies, the circle goes to the origin (for $f = 0$, $x(0) = 0, y(0) = 0$), and at high frequencies, it reaches the

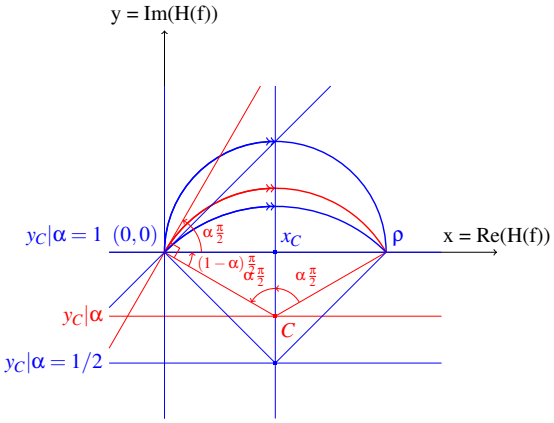

Figure 4: Theorical path of the transfer function for a high pass circuit with a CPE (circle with radius and center depending on the ratio of the resistors in the circuit and on the α parameter of the CPE).

point $(\rho,0)$ (for $f \to \infty$, $x(f) \to \frac{a}{a_*}, y(f) \to 0$). These special features are emphasized in the Nyquist plot of Fig. 4.

The angle $\alpha\frac{\pi}{2}$ is the angle between the radius crossing the x-coordinate at x_C and the radius crossing the origin. By simple geometric relations, this angle is also obtained between the tangent of the circle at the origin and the x-coordinate axis.

3.3 Comparison of Fitted Theoretical Paths With Experimental Data

Parameters of the models can be optimised to fit experimental data. Examples of fitted paths are proposed in black curves in Fig. 2 d). Table 1 gives the parameters used to fit experimental data.

Table 1: Possible fits for the parameters according to the data given in Fig. 2.

	α	ρ		α	ρ
e 1 cm	0.77	0.28	s 1 cm	0.68	0.22
e 3 cm	0.77	0.13	s 3 cm	0.68	0.12
e 5 cm	0.77	0.04	s 5 cm	0.68	0.06

The coefficient Q is set to one to describe completely the circle but appropriate fits can be made if necessary, for example by fitting special points on the path depending on the frequency.

With these parameters, it seems that the introduction of the sponge changes the order of the constant phase element as observed in Fig. 2 d). This corresponds to the shift between the electrolyte setup and the sponge setup, observed in the Bode representation of the phase angle in Fig. 2 a).

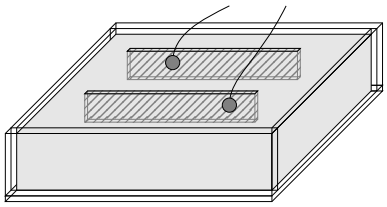

Figure 5: Experimental setup to test easily some electrodes with a sponge wet with electrolyte. Slits are cut into the sponge and electrodes are inserted inside them. The elasticity of the sponge enables to maintain electrodes in position. A PETG basin maintains the sponge and electrolyte.

4 DISCUSSION

Using platinum electrodes and low potentials enable to obtain the results presented in this study. Indeed, an important part of the study was realized with weakly golden pins for electrodes and lead to the conclusion that platinum or nobel metals with high electrochemical potentials are necessary to avoid random shifts in voltage due to reduction-oxidation reactions and lead to observable and understandable behaviors. However, in reality, EEG electrodes are sometimes weakly covered or defectuous, and this generates artefacts that are hard to correct. Understanding the model could precise the effect of these artefacts and the corrections to apply.

Concerning the choice of the medium, it is a long time since sponge are studied as elementary nervous systems, even if it is only a muscle system encapsulated in a complex body (Parker, 1919) or a more complex system in current biology (Leys et al., 1999). The conduction into these organisms is not done on a wide range, say somes centimeters. Here we tested only the conductivity induced by the structure of such an organism with synthetic sponges, not for biological purpose, but for practical one. Indeed, sponges are good for practical usage to test electroencephalographic recordings. One easy way to use them is to cut some slits with a cutter on a 1 or 2 cm depth, put some electrodes inside and fill with conductive water. The elastic structure of the sponge will maintain electrodes inside the slits and allows to test EEG recordings as in the scheme proposed in Fig. 5.

An experimental technical point that can be discussed here is that it is difficult to wash a sponge and it is hard to really clean it. A measurement of the impedance may help but the composition of the ionic elements inside the sponge is hard to evaluate. A proper model and a specific wash design must be conducted to elaborate something more precise.

Impedance spectroscopy with measurements at different frequencies can be long, but enable to control the amplitude of the simulation in order to stay in

the voltage range out of the oxydo reductive reactions.

Using white noise simulations or multiple combinations of wavelength can shorten the duration of experiments. Interestings readings about impedance spectroscopy are pointed out in (Al-Nazer et al., 2013).

The ETFE obtained from sine waves are very precise for high frequencies but are less precise for low ones. This is possibly due to the weak amplitude in the low frequencies and the presence of noise in this band. It is then hard to differentiate the tangent at the origin of the transfer function path in the Nyquist plane for the setup with electrolyte alone and the setup with the sponge. On the contrary, the ETFE obtained from white noise are more precise for low frequencies but are more contaminated by noise on high frequencies. With these ETFEs, differences of the tangents at the origin can be obtained. Some improvements of the setups can be made to improve these results.

This study can not conclude clearly on the modification of the order of the CPE and that another alternative of the proposed model can be made to fit the experimental data by taking into account a model of the electrode by a CPE in parallel with a resistor (R_p). This model is well known in litterature but with a capacitor and is proposed in (Robinson, 1968), (Ragheb and Geddes, 1990) for example. This model introduces a shift in the real part of the transfer function and the real part will tend to R_2 $(R_p + R_1 + R_2)$ for low frequency. A possible fit for the experimental data obtained with the sponge experiment, with a shift and an α set to the same value as the experiment with the electrolyte is given in Fig. 2 d) in black dashed line. With this model, the introduction of the sponge introduces a resistance in parallel with the CPE. More works have to be followed to discriminate these two models. Other appropriate methods to identify the system can be tested, with non integer exponents, like the ones proposed in (Djouambi et al., 2007), (Djouambi et al., 2012) for example.

The differences in the dispersion of the data points observed in the Nyquist plane in Fig. 2 between the electrolyte setup and the sponge setup indicate that the sponge improve the measures that are done. One hypothesis is that the sponge improves the stability of the electrodes in front of the electrolyte, in term of movements and in term of the stability of the composition of the double layer of the metal electrolyte interface. Complementary experiments must be done to precise the influence of the medium in this improvement of measures.

Another point is the equivalence of the proposed model with the different part of the experimental setup. If each electrode is modelised by a CPE, then what we observed between the input and the output of the system is the composition of two electrodes in series, then two CPE. The equivalent circuit is given in (Diard et al., 2013) and the equivalent impedance is:

$$Z_e(p) = \frac{1}{Q_1\, p^{\alpha_1}} + \frac{1}{Q_2\, p^{\alpha_2}} = \frac{1}{Q_1\, p^{\alpha_1}} \left(1 + \frac{Q_1}{Q_2\, p^{\beta}}\right)$$

where $\beta = \alpha_2 - \alpha_1$ with $\alpha_2 \geq \alpha_1$. Either the order is the same and $\beta = 0$, and an equivalent CPE of the same order is obtained with $Q_e = \frac{Q_1 Q_2}{Q_1 + Q_2}$, either one order is less than the second and this one is preponderant over the other on a given range of frequencies.

Finally, we have proposed results and discussions on the transfer functions of the system. It is possible to switch to results and discussions with the impedances, of the system, often proposed in other studies, by using Eq. (1) and making some hypotheses or tests on the value of R.

5 CONCLUSION

In this study an original system that can test the behavior of an EEG recorder observing simulated signals injected into a random medium is presented. The system is described with an electrical circuit containing a constant phase element. Equations of the transfer functions are analyzed to understand the theoretical paths followed by the transfer function in Bode or Nyquist representations. Comparison with experimental results show that the proposed system and model are pertinent for evaluating the non integer order of some constant phase elements observed in the system. Perspective of this study is the parametric recursive identification of the system using methods like in (Djouambi et al., 2012).

ACKNOWLEDGEMENTS

This project was funded in part from *Institut Rhône Alpin des Systèmes Complexes (IXXI)*. The authors would like to thank Pierre Granjon, for excellent discussions about impedance spectroscopy measurements and analyses.

REFERENCES

Al-Nazer, R., Cattin, V., Granjon, P., Montaru, M., and Ranieri, M. (2013). Broadband identification of battery electrical impedance for HEVs. *IEEE Transactions on Vehicular Technology*, 62(7):2896–2905.

Baillet, S., Riera, J. J., Marin, G., Mangin, J. F., Aubert, J., and Garnero, L. (2001). Evaluation of inverse methods and head models for EEG source localization using a human skull phantom. *Phys. Med. Biol.*, 46:77–96.

Becq, G. (2016). http://www.gipsa-lab.grenoble-inp.fr/∼guillaume.becq/projets.html Python to NI Codes. Technical report, Gipsa-lab, UMR 5216, CNRS, INPG, UGA.

Becq, G., Bienkowski, G., Diard, J.-P., and Villard, C. (2008). About MEA impedance measurement and analysis. In Rakotondrabe and Chailet, N., editors, *6th international meeting on substrate-integrated micro electrode arrays*, volume 5, pages 277–278. Springer-Verlag.

Bédard, C. and Destexhe, A. (2009). Macroscopic models of local field potentials and the apparent 1/f noise in brain activity. *Biophysics Journal*, 96(7):2589–4608.

Boonstra, T. W., Houweling, S., and Muskulus, M. (2009). Does asynchronous neuronal activity average out on a macroscopic scale ? *The Journal of Neurosciences*, 29:8871–8874.

Collier, T. J., Kynor, D. B., Bieszczad, J., Audette, W. E., Kobylarz, E. J., and Diamond, S. G. (2012). Creation of a human head phantom for testing of electroencephalography equipment and techniques. *IEEE TBME*, 59(9):2628–2634.

Cooper, R., Osselton, J. W., and Shaw, J. C. (1969). *EEG Technology*. Butterworth and co.

Dehghani, N., Bédard, C., Cash, S., Halgren, E., and Destexhe, A. (2010). Comparative power spectral analysis of simultaneous electroencephalographic and magnetoencephalographic recordings in humans suggests non-resistive extracellular media. *Journal of computational neuroscience*, pages 1–17.

Diard, J. P., Gorrec, B. L., and Montella, C. (2013). Handbook of electrochemical impedance spectroscopy. Technical report, Bio-Logic.

Didier, R. (1984). *Chimie Générale*. Technique et Documentation, Lavoisier.

Djouambi, A., Charef, A., and Voda, A. (2007). Optimal approximation, simulation and analog realization of the fundamental fractional order transfer function. *International Journal of Applied Mathematics and Computer Science*, 17(4):455–462.

Djouambi, A., Voda, A., and Charef, A. (2012). Recursive prediction error identification of fractional order models. *Communications in Nonlinear Science and Numerical Simulation*, 17(6):2517–2524.

Geddes, L. A. (1997). Historical evolution of circuit models for the electrode-electrolyte interface. *Annals of Biomedical Engineering*, 25:1–14.

Jones, E., Oliphant, E., Peterson, P., and al. (2001–2016). Scipy: Open source scientific tools for python. http://www.scipy.org/.

Jorcin, J.-J., Orazem, M. E., Pébère, N., and Tribollet, B. (2006). CPE analysis by local electrochemical impedance spectroscopy. *Electrochimica Acta*, 51(8-9):1473–1479.

Leahy, R. M., Mosher, J. C., Spencer, M., and Huang, M. L. J. D. (1998). A study of dipole localization accuracy for MEG and EEG using a human skull phantom. *Los Alamos Technical Report LA-UR-98-1442*.

Leys, S., Mackie, G., and Meech, R. (1999). Impulse conduction in a sponge. *Journal of Experimental Biology*, 202:1139–1150.

Ljung, L. (1987). *System identification : theory for the user*. Prentice-Hall.

Logothetis, N. K., Kayser, C., and Oeltermann, A. (2007). In vivo measurement of cortical impedance spectrum in monkeys: Implications for signal propagation. *Neuron*, 55(5):809–823.

Magin, R., Ortigueira, M. D., Podlubny, I., and Trujillo, J. (2011). On the fractional signals and systems. *Signal Processing*, 91(3):350–371.

Magin, R. and Ovadia, M. (2010). Modeling the cardiac tissue electrode interface using fractional calculus. *IFAC Proceedings Volumes*, 39(11):302–307.

Miller, K. J., Zanos, S., Fetz, E. E., den Nijs, M., and Ojemann, J. G. (2009). Decoupling the cortical power spectrum reveals real-time representation of individual finger movements in humans. *The Journal of Neurosciences*, 29:3132–3137.

Nunez, P. L. and Srinivasan, R. (2006). *Electric fields of the brain*. Oxford university press.

Parker, G. H. (1919). *The Elementary Nervous System*. J. B. Lipinncott Company The Washington Square Press.

Ragheb, T. and Geddes, L. A. (1990). Electrical properties of metallic electrodes. *Medical and Biomedical Engineer and Computing*, pages 182–188.

Robinson, D. A. (1968). The electrical properties of metal microelectrodes. *Proc. IEEE*, 56:1065–1071.

Schwan, H. P. and Foster, K. R. (1980). RF-field interactions with biological systems: Electrical properties and biophysical mechanisms. *Proc. IEEE*, 68(1):104–113.

Welch, P. D. (1967). The use of fast Fourier transform for the estimation of power spectra: A method based on time averaging over short modified periodograms. *IEEE TAU*, 15(2):70–73.

Zoltowski, P. (1998). On the electrical capacitance of interfaces exhibiting constant phase element behaviour. *Journal of Electroanalytical Chemistry*, 443:149–154.